DALTON

Synthesis, characterisation, and solution behaviour of two dioxomolybdenum(VI) complexes of a bis(catecholamide) siderophore analogue

Anne-Kathrin Duhme

Anorganisch-Chemisches Institut der Universität, Wilhelm-Klemm-Strasse 8, D-48149 Münster, Germany

The bis(catecholamide) α,α′-bis(2,3-dihydroxybenzoylamino)-*m*-xylene (H_4L^3) has been synthesized and characterised. It is an analogue of the naturally occurring siderophore azotochelin and structurally related to an approved enterobactin model. Two dioxomolybdenum(VI) complexes of it have been synthesized, namely a di- and a mono-nuclear one. Variable-temperature proton NMR studies of the initially obtained dinuclear compound revealed that three kinetic processes are operative in Me_2SO solution: geometrical isomerisation at lower temperatures, and inversion of configuration concomitant with dissociation into the monomer at higher temperatures. In contrast, the mononuclear complex obtained in this way isomerises and inverts almost simultaneously at 343–353 K. The crystal structure of $Na_2[MoO_2L^3]$ confirmed the mononuclear nature of the complex and revealed that the *cis*, *cis*, *cis* geometrical isomer is adopted in the solid state.

In recent years the increasing interest in the chemistry of bis(catecholates) has identified their versatile co-ordination properties.[1–8] The formation of mono- as well as di-nuclear complexes has been observed depending on the structure of the spacer between the catecholate subunits. Helicate-type dinuclear complexes are formed with octahedrally co-ordinated metal centres such as Fe^{III},[3,6] Ga^{III} [1] and Ti^{IV} [2,5] when the linking arm is too short or too rigid to allow binding of a single metal ion in a tetradentate fashion. With longer or even preoriented spacers mononuclear complexes can be formed, such as those described for Ni^{II} [7] and VO^{IV} [8] with square-planar and square-pyramidal co-ordination geometry, respectively. The alternative formation of co-ordination polymers has not been observed yet; discrete complexes are apparently entropically favoured.

Owing to the asymmetrical bidentate subunits of these compounds geometrical isomers are conceivable. Octahedral bis or tris chelate complexes can exist as either Δ or Λ optical isomers. Achiral ligands will, in general, give a racemic mixture of the two enantiomeric complexes,[2–4] but chiral ligands can direct the configuration of the metal centres to either of the two forms.[1,5,6]

My interest in bis(catecholamides) arose through their role as siderophores.[9–13] Siderophores are low-molecular-weight chelators produced by microorganisms to scavenge Fe^{III} from their local environment for transport into the cell.[14] Whereas most siderophores are hexadentate compounds capable of binding Fe^{III} in a 1:1 stoichiometric fashion, bis(bidentate) siderophores require the co-ordination of additional ligands and/or the formation of dinuclear assemblies to satisfy the preferred octahedral co-ordination geometry of Fe^{III}.[3,15] In contrast, these tetradentate compounds appear to be well suited for complexation of the MoO_2^{2+} unit, which has four vacant co-ordination sites.[16,17]

Interestingly, the type of siderophore released by the N_2-fixing cells of *Azotobacter vinelandii* is influenced by the concentration of molybdate in the growth medium.[18] In an iron-limited low-molybdate medium the bis(catecholamide) siderophore azotochelin is produced, whereas in an excess of molybdate the tris(catecholamide) protochelin [18,19] is released. Iron as well as molybdenum is a component of the conventional nitrogenase and both metals are essential for the optimal growth of *A. vinelandii*. Under normal environmental conditions molybdenum competes with iron for azotochelin, but to date there is little published information regarding molybdenum–siderophore interactions.[4,16,20–22]

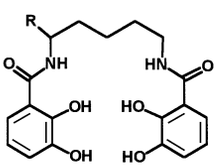

Azotochelin; R = CO_2H
H_4L^1; R = H

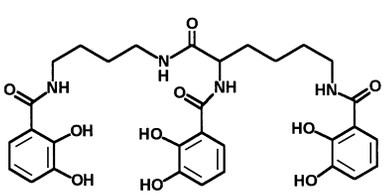

Protochelin

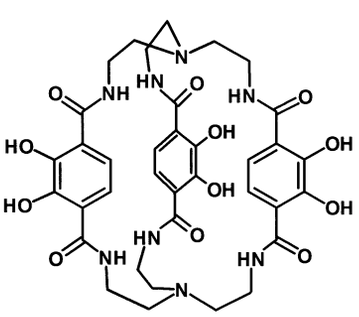

H_6L^2

In previous work it was shown that the azotochelin analogue ligand L^1 forms a dinuclear double-helical 1:1 complex with MoO_2^{2+}.[4] Yet, according to the crystal structures of the complexes $[MoO_2L^2]^{2-}$ (ref. 16) and $[NiL^1]^{2-}$ (ref. 7) a five-atom spacer separating the binding subunits should be flexible enough to allow bis(bidentate) co-ordination to just one molybdenum atom as well. In order to synthesize such a mononuclear molybdenum complex of an azotochelin analogue, we

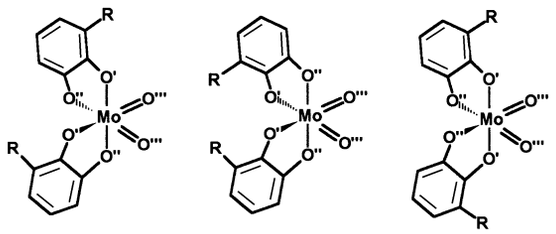

Scheme 1 Possible geometric isomers of *cis*-dioxomolybdenum(VI) complexes with two asymmetrically substituted catecholate ligands, shown in Λ configuration

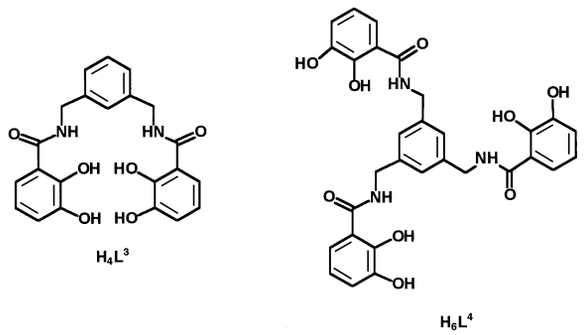

designed the model ligand L^3. This compound is structurally related to L^4, a hexadentate compound that reproduces the basic structural features of the siderophore enterobactin, one of the most powerful iron chelators known.[14]

Results and Discussion

Syntheses

The development of L^3 evolved from the following considerations. The xylene spacer not only provides the five-atom link found in the naturally occurring siderophore azotochelin, it also enhances the rigidity and preorientation of the compound and should therefore favour the encapsulation of a single MoO_2^{2+} unit. Furthermore, model studies show that steric strain in the predisposed ligand reduces the number of possible geometric isomers. For an octahedral *cis*-MoO_2^{2+} complex of an asymmetrically substituted catecholate ligand there are three conceivable geometrical isomers as shown in Scheme 1. The coordination of L^3 to the metal centre in a tetradentate fashion should give exclusively the *cis*, *cis*, *cis* isomer. In addition, the structural analogy between L^3 and L^4 appears promising for bioactivity tests: in iron-uptake studies with *Escherichia coli* the enterobactin analogue L^4 was observed to promote the growth of auxotroph mutants.[14]

The compound H_4L^3 was synthesized in a two-step procedure by reaction of 2,3-dimethoxybenzoic acid with α,α′-diamino-*m*-xylene *via* *N*,*N*′-carbonyldiimidazole coupling (76% yield), followed by deprotection of the hydroxyl groups with BBr_3. It could be crystallised from water–methanol at pH-meter reading 7.0 (95% yield). Stoichiometric reaction of an aqueous Na_2MoO_4 solution with a solution of H_4L^3 in methanol resulted in the formation of a soluble molybdenum complex which was isolated as the orange powder $Na_4[(MoO_2L^3)_2]$ **1** by slow precipitation with tetrahydrofuran (thf)–Et_2O.

Elemental analysis of the dried powder **1** is consistent with the expected 1:1 complex $[MoO_2L^3]^{2-}$. However, mass spectrometry showed an isotope distribution pattern and small additional peaks associated with a 2:2 complex $[(MoO_2L^3)_2]^{4-}$. This suggests that the product might be a dinuclear compound. Further evidence for the existence of a dimeric species was provided by a molecular-weight distribution analysis of the $[NMe_4]^+$-salt

Table 1 Selected bond lengths (Å) and angles (°) for $Na_2[MoO_2L^3]\cdot 3Me_2SO$ with estimated standard deviations in parentheses. Symmetry codes I $-x, -y+1, z+1$; II $x, y-1, z$; III $-x, -y, -z$; IV $x, y+1, z$; V $-x, -y, -z+1$; VI $-x, -y+1, -z$. Atoms O(9)–O(11) correspond to those of Me_2SO molecules

Mo–O(1)	1.707(2)	Na(1)–O(7^{III})	2.433(2)
Mo–O(2)	1.734(2)	Na(1)–O(10^{III})	2.455(2)
Mo–O(3)	1.998(2)	Na(1)–O(1^{II})	2.981(2)
Mo–O(4)	2.186(2)	Na(2)–O(11^{I})	2.301(2)
Mo–O(5)	2.125(2)	Na(2)–O(2)	2.340(2)
Mo–O(6)	2.012(2)	Na(2)–O(10^{VI})	2.358(2)
Na(1)–O(9)	2.315(2)	Na(2)–O(4^{I})	2.413(2)
Na(1)–O(8)	2.391(2)	Na(2)–O(2^{I})	2.575(2)
Na(1)–O(11^{V})	2.431(2)	Na(2)–O(6^{I})	2.644(2)
O(1)–Mo–O(2)	101.87(9)	O(2)–Mo–O(6)	87.83(8)
O(1)–Mo–O(3)	91.33(8)	O(3)–Mo–O(4)	75.28(7)
O(1)–Mo–O(4)	166.48(7)	O(3)–Mo–O(5)	82.71(7)
O(1)–Mo–O(5)	92.37(8)	O(3)–Mo–O(6)	151.40(7)
O(1)–Mo–O(6)	108.37(8)	O(4)–Mo–O(5)	84.19(7)
O(2)–Mo–O(3)	108.68(8)	O(4)–Mo–O(6)	83.55(7)
O(2)–Mo–O(4)	84.55(8)	O(5)–Mo–O(6)	76.13(7)
O(2)–Mo–O(5)	161.32(7)		

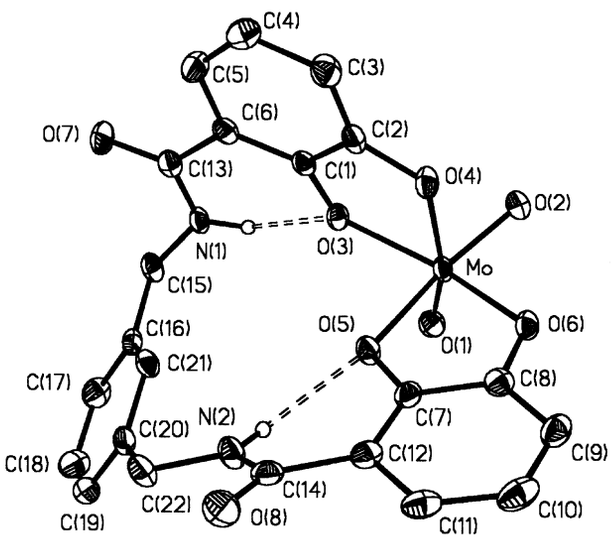

Fig. 1 Structure of the anion of $[MoO_2L^3]^{2-}$ **2** showing the atom labelling scheme. For clarity only the protons at N(1) and N(2) are included

of the complex by gel filtration (Sephadex LH-20, methanol).* Apart from a major fraction corresponding to the dimeric species, a second band was eluted which could be assigned to a monomer. As reanalysis of the major fraction gave the same result, a conversion of **1** into a monomeric species is evidently occurring in solution. The dissociation of **1** could be monitored by NMR spectroscopy in $(CD_3)_2SO$ since the differences in the chemical shifts of the NH protons are large enough to allow detection of the bridging ligand in the dimer in the presence of the chelating ligand in the monomer (see NMR section). The conversion is slow at room temperature, but the dissociation is almost quantitative after heating a 25 mmol dm^{-3} solution of **1** in $(CD_3)_2SO$ to 353 K for 5 h. Although the rate can be enhanced by increasing the temperature or the concentration

* Unfortunately, aqueous solutions of complex **1** containing sodium counter ions were not suitable for molecular-weight determinations as elution was retarded, due to interactions between the cations, the gel and the complex anions. The complexes Ferrichrome A, $[FeL^4]^{3-}$, $[MoO_2(cat)_2]^{2-}$ (H_2cat = catechol) and [Fe(malt)$_3$] [Hmalt = maltol, 3-hydroxy-2-methyl-(4*H*)-pyran-4-one] were used as markers to calibrate the column.

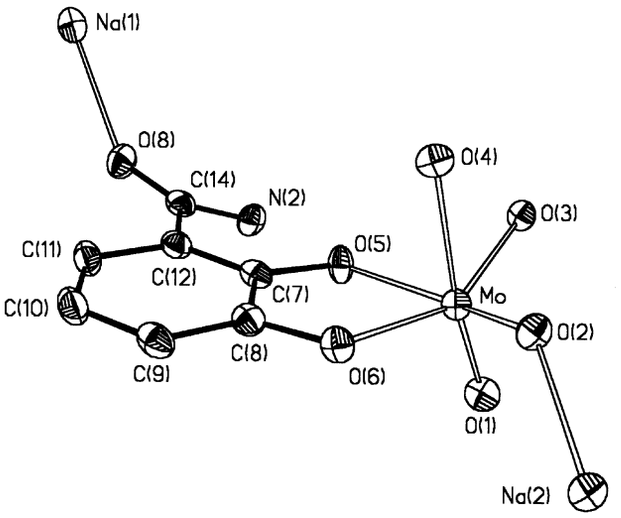

Fig. 2 Detail of the inner co-ordination sphere of Mo(1) and the geometry of the distorted binding subunit

the conditions stated above proved optimal for the crystallisation of $Na_2[MoO_2L^3]$ **2**.

Crystal structure of $Na_2[MoO_2L^3]\cdot 3Me_2SO$

Orange X-ray-quality crystals were obtained as described in the Experimental section; recrystallisation was unnecessary. The crystal structure proves conclusively that complex **2** consists of discrete mononuclear dianions connected through a network of sodium counter ions and co-ordinated Me_2SO molecules. The structure of the complex anion is shown in Fig. 1 and selected bond lengths and angles are listed in Table 1.

As in $[(MoO_2L^1)_2]^{4-}$,[4] and as predicted by model studies, the *cis*, *cis*, *cis* geometric isomer is formed in which the two binding subunits are oriented differently: in one subunit the catecholate oxygen *ortho* to the amide substituent [O(5)] is bound *trans* to the oxo ligand [O(2)] while in the other the atom positioned *meta* to the amide moiety [O(4)] is oriented *trans* to the oxo ligand [O(1)].

The geometry around the molybdenum atom is distorted octahedral with angles in the ranges 75–109 and 151–167°. The dioxomolybdenum unit adopts the usual *cis* arrangement with the Mo=O distances being markedly different. This difference reflects the stronger involvement of the oxo ligand O(2) in the co-ordination sphere of Na(2) [2.340(2) Å] than the participation of O(1) in the binding of Na(1) [2.981(2) Å]. The result of this stronger interaction is not only a lengthening of the Mo–O(2) double bond [1.734(2) Å] but also a shortening of the Mo–O(5) single bond [2.125(2) Å] in *trans* position, because of the diminished *trans* influence of the oxo ligand O(2). In comparison, the Mo–O(4) single bond [2.186(2) Å] is significantly longer, due to the additional interaction of O(4) with the counterion Na(2) [2.413(2) Å]. Since the Mo=O(1) bond [1.707(2) Å] is shortened correspondingly, the resulting average Mo=O distance of 1.721 Å is very similar to the 1.718 Å observed for $[(MoO_2L^1)_2]^{4-}$.[4]

The coplanar arrangement of the catechol rings and the amide functions usually observed in catecholamide complexes[23] is distorted in this case by the steric strain of the rigid ligand L^3. The amide group is rotated out of the plane of its associated aromatic ring by 9.3(2)° for N(1) and 22.4(3)° for N(2). The pronounced distortion in the latter case can also be explained by electronic effects exerted by the co-ordinated sodium counter ions (Fig. 2). The strengthening of the Mo–O(5) bond as a consequence of the co-ordination of Na(2) to O(2) further affects the intramolecular hydrogen-bonding pattern. While the slightly stronger hydrogen bond between the catecholate oxygen O(3) and its adjacent amide hydrogen helps to lock the corresponding subunit in a planar configuration [d(N···O) = 2.659(3) Å], the weaker hydrogen bond between O(5) and H(2) allows a higher degree of distortion from planarity [d(N···O) = 2.740(3) Å]. In addition, Na(1) is bound more strongly to the carbonyl oxygen atom O(8) than to O(7), thereby interfering differently with the aromatic amide π networks, which help to hold the unit in a planar array.

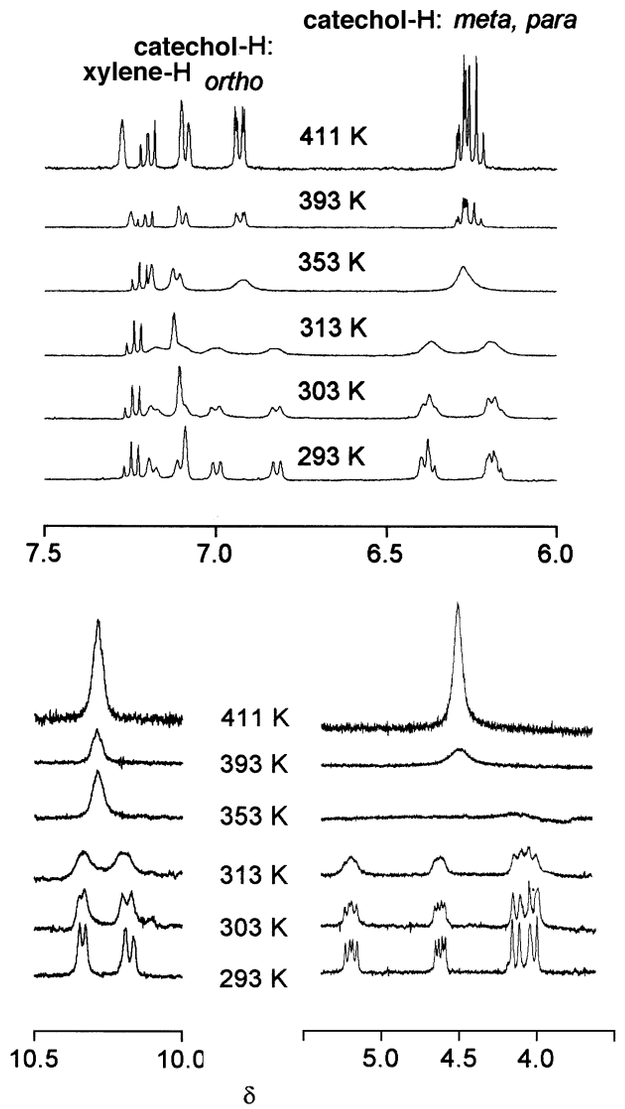

Fig. 3 Variable-temperature proton NMR spectra of complex **2**, shown in the aromatic region (above) and the NH and CH_2 regions, respectively (below)

Proton NMR spectroscopy

The room-temperature NMR data for H_4L^3 and the molybdenum complexes **1** and **2** are given in the Experimental section. Compared with free H_4L^3 the spectra of **1** and **2** show complex splittings. In part, this results from the geminal benzylic protons, which are diastereotopic because the metal centres are chiral: the complexes form a racemic mixture of the enantiomeric Δ and Λ forms in solution. Furthermore, the formation of the *cis*, *cis*, *cis* geometric isomer (Scheme 1), in which the two binding subunits are inequivalent, gives rise to two sets of proton resonances.

In contrast to the sharp signals in the ^{1}H NMR spectrum of complex **2**, the resonances in the spectrum of **1** suffer significantly from exchange broadening, indicating non-rigid behaviour at room temperature. Complexes having a $MoO_2(L–L')_2$ structure can exhibit two types of stereochemical non-rigidity: inversion and geometrical isomerisation.[24] In order to

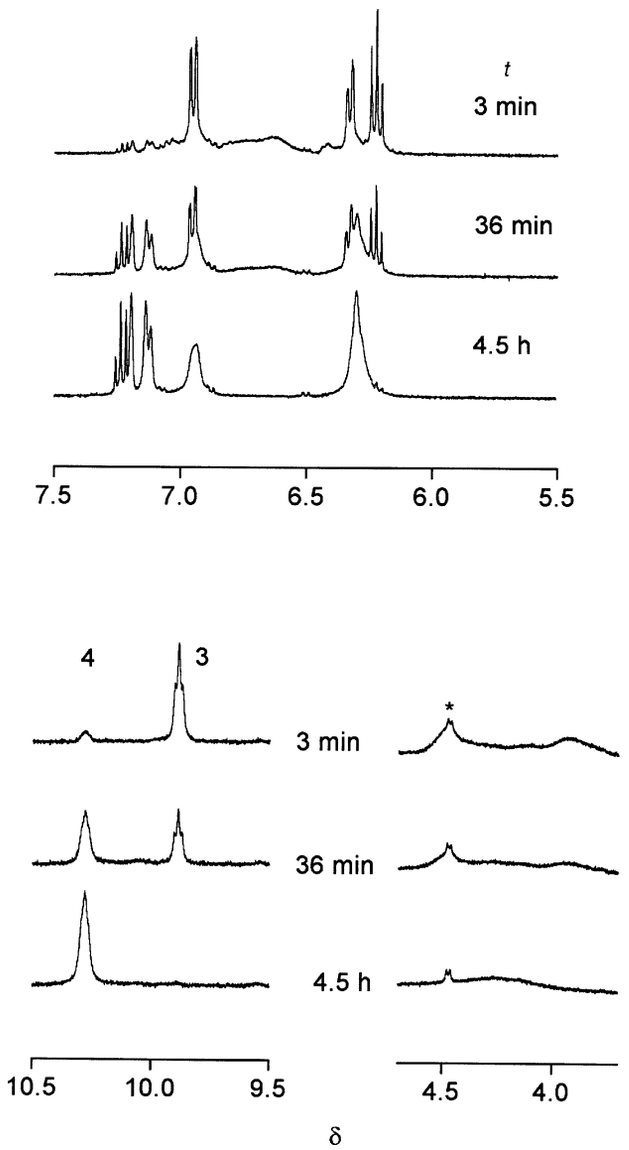

Fig. 4 Proton NMR spectra recorded at 353 K during the course of the conversion of complex **1** into **2**, 50 mmol dm^{-3} molybdenum; the asterisk indicates free H_4L^3 or unco-ordinated 'dangling' subunit

investigate these two processes variable-temperature NMR studies were conducted on both **1** and **2**. The aromatic protons of the catechol subunits were monitored in order to follow geometrical isomerisation, while the diastereotopic benzylic protons provided supplementary sensors for the inversion of configuration.

A set of selected spectra of complex **2** in $(CD_3)_2SO$ over the temperature range 293–411 K is presented in Fig. 3. Upon heating the signals assigned to the aromatic catecholate protons progressively broaden, coalesce at 343 K ($\Delta G^{\ddagger} = 70$ kJ mol^{-1}, calculated for H_{ortho}), and resolve into a single set of sharp signals at 411 K. The same activation barrier for the isomerisation is calculated from the averaging of the NH protons. The inversion seems to occur simultaneously: the geminal coupling of the diastereotopic benzylic protons collapses at approximately 353 K, which also gives an estimated activation barrier for inversion of configuration of 70 kJ mol^{-1}. Simultaneous isomerisation and inversion could either proceed intramolecularly through a Ray–Dutt twist or through a bond-rupture mechanism involving a five-co-ordinate transition state.[24] Although the spectra do not allow a distinction between the two mechanisms, the strong *trans* influence of the oxo-ligands should favour a rupture of the Mo–O single bonds in *trans* position.

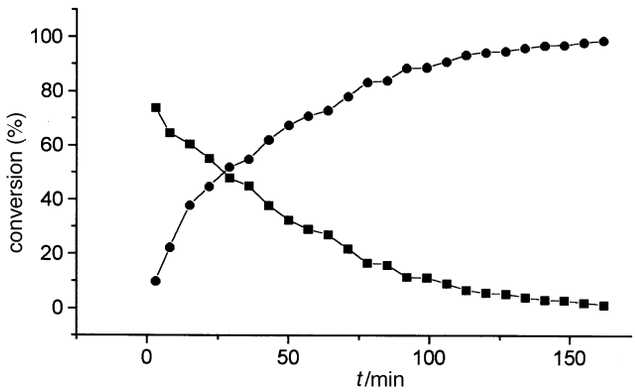

Fig. 5 Reaction profile for the conversion of $[(MoO_2L^3)_2]^{4-}$ (■) into $[MoO_2L^3]^{2-}$ (●) determined by integration of the amide proton resonances, 50 mmol dm^{-3} Mo, solvent Me_2SO, $T = 353$ K. Data points are the average values for two kinetic runs

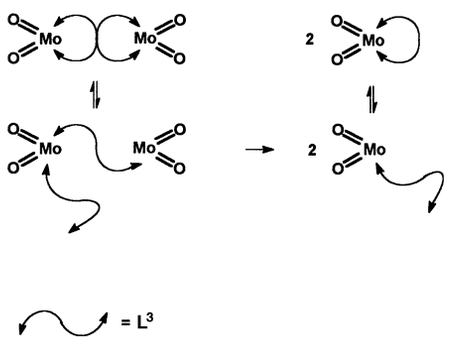

Scheme 2 Schematic representation of a conceivable mechanism for the dissociation of complex **1**, showing intermediates with unco-ordinated 'dangling' subunits

The solution behaviour of complex **1** is somewhat different. The variable-temperature spectra reveal three kinetic processes. In the lower part of the temperature range the operative process is the isomerisation. Unfortunately, activation parameters could not be obtained, since it was not possible to reach the slow-exchange region using Me_2SO as solvent. The second process is the inversion of configuration, which begins to operate in a temperature range where the geometrical isomerisation at the metal centres is already fast. The first spectrum shown in Fig. 4 ($t = 3$ min) is essentially the one of isomer **1** at 353 K, although a minor amount of **2** is present. The aromatic protons of the catecholate units exhibit only one set of sharp signals at this temperature indicating rapid isomerisation. The signals of the diastereotopic CH_2 protons still appear as two (although broad) signals. Their coalescence point is reached after further heating at 383 K. The resulting activation barrier of $\Delta G^{\ddagger} = 75$ kJ mol^{-1} is very similar to that obtained for the mononuclear complex **2**. This is in accordance with the observation that dinuclear gallium–catecholamide helicates have free-energy inversion barriers similar to those of comparable mononuclear complexes.[25] Interestingly, distinct low-temperature isomerisation and high-temperature inversion has also been observed for the dinuclear $[(MoO_2L^1)_2]^{4-}$ complex[4] and may be a common feature for this type of dimeric catecholamide complexes.

The third process is the conversion of complex **3** into the mononuclear **2**. At 353 K and 50 mmol dm^{-3} molybdenum 50% conversion is reached within 36 min, as is evident from Figs. 4 and 5. The experimental data shown in Fig. 5 have not been fitted by an explicit kinetic function since a number of consecutive steps have to be taken into account as outlined in Scheme 2. Maybe even additional parallel pathways are operative, similar to those postulated for iron(III) dihydroxamate complexes.[26] After 4.5 h the dissociation is essentially

complete and the final proton NMR spectrum is almost identical that of **3** at the same temperature. The reaction is not reversible on cooling, probably due to the rigidity of the ligand. The fact that the monomerisation inevitably involves ligand dissociation (Scheme 2) confirms that bond cleavages definitely occur in the present system.

Experimental

General methods

Commercially available reagents (Aldrich, Fluka) were used without further purification. Tetrahydrofuran and dichloromethane were distilled from sodium–benzophenone and lithium aluminium hydride, respectively. The NMR data were recorded on Bruker AM-300, -360 and -400 spectrometers. Acetone was used as a standard to calibrate the variable-temperature spectra. Melting points were determined on a Kofler micro-hotplate combined with a Reichert-Jung transformer and are uncorrected. The IR spectra were recorded using a Bruker IFS 113 v spectrometer. Elemental analyses were performed by the Microanalytical Service, and mass spectra recorded by the Mass Spectrometry Laboratory, both of the Organic Chemistry Department, University of Münster.

Syntheses

α,α′-Bis(2,3-dimethoxybenzoylamino)-*m*-xylene. Solid *N*,*N*′-carbonyldiimidazole (4.866 g, 30.00 mmol) was added to a solution of 2,3-dimethoxybenzoic acid (5.466 g, 30.00 mmol) in anhydrous thf (30 cm^3). After evolution of CO_2 had ceased a solution of α,α′-diamino-*m*-xylene (1.95 cm^3, 15.00 mmol) in thf (15 cm^3) was added dropwise over 3 h to the vigorously stirred solution. The reaction mixture was stirred at room temperature for 24 h. After solvent evaporation the resulting residue was dissolved in $CHCl_3$ and washed with 2 mol dm^{-3} HCl, saturated $NaHCO_3$ solution, and three times with water. After drying over $MgSO_4$, removal of the solvent *in vacuo* afforded an oil which solidified upon standing. Recrystallisation from ethyl acetate–hexanes gave white crystals (5.296 g, 76%), m.p. 98 °C (Found: C, 67.0; H, 6.05; N, 5.9%; M^+, 465. $C_{26}H_{28}N_2O_6$ requires C, 67.2; H, 6.05; N, 6.0%; *M*, 465); δ_H(300 MHz, $CDCl_3$) 3.76 (6 H, s, 2 CH_3), 3.79 (6 H, s, 2 CH_3), 4.60 (4 H, d, *J* 5.6, 2 CH_2), 6.97 (2 H, d, *J* 8.0, 2 aromatic H), 7.06 (2 H, t, *J* 7.9, 2 aromatic H), 7.63 (2 H, d, *J* 7.9 Hz, 2 aromatic H) and 8.29 (2 H, br s, 2 NH).

α,α′-Bis(2,3-dihydroxybenzoylamino)-*m*-xylene H_4L^3. A solution of the above compound (2.323 g, 5.00 mmol) in degassed dry CH_2Cl_2 (25 cm^3) was added dropwise to a 1 mol dm^{-3} solution (50 cm^3) of BBr_3 in CH_2Cl_2 at 0 °C under argon. The resulting white suspension was stirred at room temperature overnight, water (40 cm^3) was carefully added (HBr evolution) and the mixture stirred for 2 h to ensure complete hydrolysis. The precipitate was filtered off, washed with water and dissolved in methanol. The solvent was evaporated three times to remove boron compounds and the residue finally recrystallised from methanol–water at pH-meter reading 7.0 to give H_4L^3 as white needles (1.940 g, 95%), m.p. 172 °C (Found: C, 64.4; H, 4.8; N, 6.6%; M^+, 408. $C_{22}H_{20}N_2O_6$ requires C, 64.7; H, 4.9; N, 6.9%; *M*, 408); δ_H[400 MHz, $(CD_3)_2SO$] 4.51 (4 H, d, *J* 5.5, 2 CH_2), 6.69 (2 H, t, *J* 7.9, 2 aromatic H), 6.94 (2 H, d, *J* 7.6, 2 aromatic H), 7.23–7.33 (4 H, m, 4 aromatic H), 7.36 (2 H, d, *J* 7.9, 2 aromatic H) and 9.37 (2 H, t, *J* 5.5 Hz, 2 NH).

$Na_4[(MoO_2L^3)_2]$ 1. A solution of H_4L^3 (1.430 g, 3.50 mmol) in methanol (10 cm^3) was added to a solution of $Na_2MoO_4 \cdot 2H_2O$ (0.848 g, 3.50 mmol) in water (5 cm^3). The resulting clear orange solution was overlayered with thf and diethyl ether. After standing overnight at room temperature the resultant orange precipitate was filtered off, washed with thf, and dried *in vacuo*. Yield: 1.237 g (61%) {Found: C, 42.0; H, 3.65; N, 4.3%; matrix-assisted laser desorption ionisation mass spectrum with 2,3-dihydroxobenzoic acid matrix $(Na[M])^{2+}$ *m*/*z* 555 ($Na[M]^{2+}$) and 1087 ($Na[M]^+$). $C_{44}H_{32}Mo_2N_4Na_4O_{16} \cdot 6H_2O$ requires C, 41.8; H, 3.6; N, 4.4%}; $\tilde{\nu}_{max}/cm^{-1}$ (KBr) 867 and 898 (*cis*-MoO_2); δ_H[300 MHz, $(CD_3)_2SO$, cat = catecholate, xyl = xylene] 3.77 (1 H, br d, *J* 13.3, 0.5 CH_2), 3.98 (1 H, br d, *J* 14.4, 0.5 CH_2), 4.45 (1 H, br d, *J* 13.3, 0.5 CH_2), 4.50 (1 H, br d, *J* 14.4, 0.5 CH_2), 6.23 (1 H, t, *J* 7.5, 1 aromatic cat H), 6.24 (1 H, t, *J* 7.5, 1 aromatic cat H), 6.34 (1 H, d, *J* 7.4, 1 aromatic cat H), 6.36 (1 H, d, *J* 7.4, 1 aromatic cat H), 6.42 (1 H, br s, 1 aromatic xyl H), 6.63 (1 H, t, *J* 7.5, 1 aromatic xyl H), 6.73 (1 H, br m, 1 aromatic xyl H), 6.88 (1 H, br s, 1 aromatic xyl H), 6.96 (2 H, d, *J* 7.9 Hz, 2 aromatic cat H) and 9.94 (2 H, br s, 2 NH).

$Na_2[MoO_2L^3]$ 2. A solution of complex **1** (632 mg, 0.50 mmol) in Me_2SO (20 cm^3) was stirred and heated at 80 °C overnight with exclusion of moisture. After filtration the solution was overlayered first with thf and secondly with Et_2O, and then chilled to 5 °C. The orange crystals obtained were stable only in equilibrium with their mother-liquor or, if isolated, at low temperature (<20 °C). Storage under other conditions led to the formation of a red oil. Yield: 390 mg (48%) (Found: C, 41.8; H, 4.0; N, 3.3. $C_{22}H_{16}MoN_2Na_2O_{11} \cdot 3C_6H_{18}O_3S_3$ requires C, 41.4; H, 4.2; N, 3.45%); $\tilde{\nu}_{max}/cm^{-1}$ (KBr) 857 and 895 (*cis*-MoO_2); δ_H[300 MHz, $(CD_3)_2SO$], 4.11 (1 H, d, J_{HH} = 15.9, J_{HNH} = 0.0, 0.5 CH_2), 4.22 (1 H, d, J_{HH} = 16.0, J_{HNH} = 0.0, 0.5 CH_2), 4.72 (1 H, dd, J_{HH} = 15.9, J_{HNH} = 7.6, 0.5 CH_2), 5.29 (1 H, dd, J_{HH} = 16.0, J_{HNH} = 10.0, 0.5 CH_2), 6.28 (2 H, m, 2 aromatic cat H), 6.47 (2 H, m, 2 aromatic cat H), 6.91 (1 H, d, *J* 7.8, 1 aromatic cat H), 7.09 (1 H, d, *J* 8.0, 1 aromatic cat H), 7.28–7.38 (4 H, m, 4 aromatic xyl H), 10.27 (1 H, d, J_{HNH} = 10.0, NH) and 10.43 (1 H, d, J_{HNH} = 7.6 Hz, NH).

Crystallography

X-Ray-quality crystals of complex **2** were obtained as described above. A fragment was cut, mounted on a glass capillary and cooled under a stream of nitrogen.

Crystal data and data collection parameters. $C_{28}H_{34}MoN_2Na_2O_{11}S_3$, $M = 812.7$, orange fragment (0.07 × 0.17 × 0.2 mm), triclinic, space group $P\bar{1}$ (no. 2), $a = 11.498(2)$, $b = 11.720(2)$, $c = 13.079(3)$ Å, $\alpha = 84.09(3)$, $\beta = 74.76(3)$, $\gamma = 79.30(3)°$, $U = 1668.2(6)$ $Å^3$, $Z = 2$, $D_c = 1.618$ g cm^{-3}, $F(000) = 832$, $\mu = 6.7$ cm^{-1}, $T = 170$ K, Siemens-P3 diffractometer, graphite-monochromated Mo-Kα radiation ($\lambda = 0.710\,73$ Å), ω–2θ scan mode, no absorption correction, 7638 reflections measured ($4.3 < 2\theta < 54.0°$, $+h, \pm k, \pm l$), 7269 unique ($R_{int} = 0.022$), 5783 observed [$I > 2\sigma(I)$].

Structure solution and refinement. The structure was solved by direct methods by means of the SHELXS 86 program.[27] The refinement on F^2 was carried out by full-matrix least squares (SHELXL 93)[28] with 430 free parameters and 7262 reflections to a final $R1 = 0.031$, $wR2 = 0.072$ [for reflections with $I > 2\sigma(I)$], and 0.045 and 0.091 (for all reflections); the weighting scheme was $w = 1/[\sigma^2(F_o^2) + (0.0387P)^2]$ where $P = (F_o^2 + 2F_c^2)/3$ and goodness of fit = 0.98. Hydrogen atoms of the organic ligand were included in the refinement in calculated positions, non-hydrogen atoms were refined anisotropically.

Atomic coordinates, thermal parameters, and bond lengths and angles have been deposited at the Cambridge Crystallographic Data Centre (CCDC). See Instructions for Authors, *J. Chem. Soc.*, *Dalton Trans.*, 1997, Issue 1. Any request to the CCDC for this material should quote the full literature citation and the reference number 186/367.

Acknowledgements

This work was supported by the Deutsche Forschungsgemeinschaft and the Fonds der Chemischen Industrie. I thank M. Läge for the crystallographic data collection, K. Busse for the variable-temperature NMR measurements, and Professors R. C. Hider and B. Krebs for helpful discussions.

References

1 E. J. Enemark and T. D. P. Stack, *Angew. Chem., Int. Ed. Engl.*, 1995, **34**, 996.
2 M. Albrecht and S. Kotila, *Angew. Chem., Int. Ed. Engl.*, 1995, **34**, 3134; 1996, **35**, 1208.
3 E. J. Enemark and T. D. P. Stack, *Inorg. Chem.*, 1996, **35**, 2719.
4 A.-K. Duhme, Z. Dauter, R. C. Hider and S. Pohl, *Inorg. Chem.*, 1996, **35**, 3059.
5 M. Albrecht, *Synlett*, 1996, 565.
6 B. Kersting, M. Meyer, R. E. Powers and K. N. Raymond, *J. Am. Chem. Soc.*, 1996, **118**, 7221.
7 S.-P. Huang, K. J. Franz, M. M. Olmstead and R. H. Fish, *Inorg. Chem.*, 1995, **34**, 2820.
8 T. M. Dewey, J. Du Bois and K. N. Raymond, *Inorg. Chem.*, 1993, **32**, 1729.
9 J. L. Corbin and W. A. Bulen, *Biochemistry*, 1969, **8**, 757.
10 G. H. Tait, *Biochem. J.*, 1975, **146**, 191.
11 S. Yamamoto, N. Okujo, Y. Fujito, M. Saito, T. Yoshida and S. Shimoda, *J. Biochem.*, 1993, **113**, 538.
12 G. Ehlert, K. Taraz and H. Budzikiewicz, *Z. Naturforsch., Teil C*, 1994, **49**, 11.
13 J. R. Telford, J. A. Leary, L. M. G. Tunstad, B. R. Byers and K. N. Raymond, *J. Am. Chem. Soc.*, 1994, **116**, 4499.
14 R. C. Hider, *Struct. Bonding* (*Berlin*), 1984, **58**, 26; K. N. Raymond, G. Müller and B. F. Matzanke, *Top. Curr. Chem.*, 1984, **123**, 49.
15 R. C. Scarrow, D. L. White and K. N. Raymond, *J. Am. Chem. Soc.*, 1985, **107**, 6540.
16 M. Albrecht, S. J. Franklin and K. N. Raymond, *Inorg. Chem.*, 1994, **33**, 5785.
17 W. P. Griffith, H. I. S. Nogeira, B. C. Parkin, R. N. Sheppard, A. J. P. White and D. J. Williams, *J. Chem. Soc., Dalton Trans.*, 1995, 1775.
18 A. S. Cornish and W. J. Page, *Biol. Met.*, 1995, **8**, 332.
19 K. Taraz, G. Ehlert, K. Geisen, H. Budzikiewicz, H. Korth and G. Pulverer, *Z. Naturforsch., Teil B*, 1990, **45**, 1327.
20 A.-K. Duhme, R. C. Hider and H. Khodr, *Biol. Met.*, 1996, **9**, 245.
21 U. Patel, M. D. Baxi and V. V. Modi, *Curr. Microbiol.*, 1988, **17**, 179.
22 B. Saxena, L. Vithlani and V. V. Modi, *Curr. Microbiol.*, 1989, **19**, 291.
23 T. M. Garett, M. E. Cass and K. N. Raymond, *J. Coord. Chem.*, 1992, **25**, 241.
24 R. H. Holm, in *Stereochemically Nonrigid Metal Chelate Complexes in Dynamic NMR*, eds. L. M. Jackman and F. A. Cotton, Academic Press, New York, 1974, ch. 9, pp. 317–376.
25 B. Kersting, J. R. Telford, M. Meyer and K. N. Raymond, *J. Am. Chem. Soc.*, 1996, **118**, 5712.
26 M. T. Caudle, L. P. Cogswell and A. L. Crumbliss, *Inorg. Chem.*, 1994, **33**, 4759.
27 G. M. Sheldrick, SHELXS 86, University of Göttingen, 1986.
28 G. M. Sheldrick, SHELXL 93, University of Göttingen, 1993.

Received 21*st October* 1996; *Paper* 6/07163E